Random pseudobinary ionic alloys: lattice energy and structural properties

1997 J. Phys.: Condens. Matter 9 11141

(http://iopscience.iop.org/0953-8984/9/50/015)

J. Phys.: Condens. Matter **9** (1997) 11141–11149. Printed in the UK PII: S0953-8984(97)86829-4

Random pseudobinary ionic alloys: lattice energy and structural properties

U Tinivella†§, M Peressi‡ and A Baldereschi†‡

† Institut de Physique Appliquée, Ecole Polytechnique Fédérale de Lausanne, PHB-Ecublens, CH-1015 Lausanne, Switzerland

‡ Instituto Nazionale di Fisica della Materia (INFM)–Dipartimento di Fisica Teorica dell'Università di Trieste, Strada Costiera 11, I-34014, Italy

Received 13 August 1997

Abstract. Experimental data suggest that in ionic solid solutions the bond-length mismatch is partially accommodated by microscopic lattice distortions. In this paper we study the structural properties of ionic alloys using a generalized Born–Mayer energy model accounting for the possibility of atomic-scale relaxations. Cubic supercells are used to simulate the real random alloys, providing statistical information about the atomic distribution and interatomic distances. The good agreement with the available experimental data and with the results of *ab initio* pseudopotential calculations performed for comparison for some selected systems indicate the validity of the model here employed. We also discuss the applicability to ionic alloys of the *special quasi-random structures* originally proposed for semiconducting alloys.

1. Introduction

The extended x-ray absorption fine structure (EXAFS) technique has been successfully applied to study the atomic-scale structure of many crystalline solid solutions, and in particular of some ionic pseudobinary alloys $A_{1-x}B_xC$, both common anion (such as $K_{1-x}Rb_xBr$ [1, 2], $K_{1-x}Na_xCl$, and $K_{1-x}Na_xBr$ [3]) and common cation ($RbBr_{1-x}I_x$ [1], $RbBr_xCl_{1-x}$ [2, 4], and $KCl_{1-x}Br_x$ [5]). The main results that appear from the analysis of EXAFS data are the following: (i) the nearest-neighbour (NN) distances follow a bimodal distribution with average values that, for a given concentration, are intermediate between those of the corresponding pure compound and the linear interpolation between the two values of the pure compounds (Vegard's law) [6]; (ii) for each composition, the weighted average of the two different average NN distances is close to the Vegard value, and hence to that corresponding to the average lattice parameter of the alloy measured by x-ray; (iii) the next-nearest-neighbour (NNN) distances follow a more complicated distribution with three or four relevant peaks.

Much theoretical effort has been devoted in the past to interpreting the experimental data concerning the average lattice parameter and the enthalpy of mixing [7] with simple theories describing the alloy as a uniform average medium. Less effort conversely has been made to study the internal lattice relaxations, which, according to the experimentally observed different interatomic distances, should be present in the alloys. To our knowledge, the only attempt in this direction was proposed by Maity *et al* [8], who described the variation of

§ Present address: Osservatorio Geofisico Sperimentale, Borgo Grotta Gigante, I-34016 Trieste, Italy.

0953-8984/97/5011141+09$19.50

the NN distances with the composition in terms of few parameters derived from the pure compounds. A simple cluster model considering the mixed crystal made up of domains of pure compounds in contact with each other has been recently proposed to explain the observed x-ray absorption near-edge structure spectra of $K_{1-x}Na_xCl$ [9]. Other theoretical models are available to explain the lattice relaxation around isolated impurities [10].

More recently, Frenkel *et al* [2] performed a molecular-dynamic simulation for two selected alloys (namely, $Rb_{0.76}K_{0.24}Br$ and $RbBr_{0.62}Cl_{0.38}$) described by a 10^3-atom cluster with random occupation of the mixed sublattice, assuming harmonic potentials between NN pairs, with force constants derived from the pure compounds and equilibrium bond lengths taken equal to the average lengths of A–C and B–C bonds experimentally determined in the alloy. After the simulation, the resulting average equilibrium NN distances are not dissimilar from the input values used in the harmonic pair potential.

At variance with this approach, our aim is to implement a model which—making use of bulk parameters only and not requiring further experimental inputs—is completely transferable to alloys of any composition and which predicts NN bond lengths, average lattice parameters, and heats of formation with a very limited computational effort. With this aim a simple model accounting for atomic-scale relaxations was proposed a few years ago by some of the present authors [11]. Periodically repeated supercells are used to describe the alloys, whose energy is evaluated using a generalized Born–Mayer model, originally formulated for pure compounds [12]. Application of the model to those alloys for which experimental data were available gave promising results, despite the very small size of the simulation supercell [11]. Here we better exploit the power of the model, applying it to larger supercells of various shapes, sizes, and fillings in corresponding to a wide range of alloy compositions. The use of larger supercells filled according to cubic symmetry (as proposed in the original version of the model), randomly, or, even better, according to the so-called *special quasi-random structures* (SQSs) (proposed by Zunger *et al* [13] and successfully applied mainly to study the electronic properties of covalent alloys) allows for a satisfactory simulation of the real disordered systems and provides some statistics about the distribution of the interatomic distances.

In the next section we present the generalized Born–Mayer model, and we describe the supercells used. In section 3 we present the applications to $K_{1-x}Rb_xBr$ and show the results obtained, comparing them with available experimental data. In the last section we discuss the application of our model to other ionic alloys, we compare the results with *ab initio* pseudopotential calculations performed for some selected systems, and we draw our conclusions.

2. The model

As already proposed in [11] we use a simple form of the Born–Mayer model [12] to calculate the lattice energy, including three terms:

$$\begin{aligned}\mathcal{E} &= \mathcal{E}_{coul.} + \mathcal{E}_{rep.} + \mathcal{E}_{pol.} \\ &= \frac{1}{2}\sum_{i\neq j}\frac{Z_i Z_j e^2}{r_{ij}} + \frac{1}{2}\sum_{i,j}^{(NN)} B_{ij}\,\mathrm{e}^{-r_{ij}/\rho_{ij}} - \sum_i \alpha_i |\boldsymbol{E}(r_i;\{r_j;Z_j\})|^2 \end{aligned} \tag{1}$$

where $\boldsymbol{r}_i$, Z_i, and α_i are respectively the ionic position, charge, and polarizability of the ith ion, and $r_{ij} = |\boldsymbol{r}_i - \boldsymbol{r}_j|$. The first term is the Madelung sum of the electrostatic charge–charge interactions between the ions; the second is the repulsive energy, including the short-range repulsive interactions between NN pairs only; the last term is the polarization energy, given

by the sum of the interactions of the ionic dipole $\alpha_i \boldsymbol{E}(r_i; \{r_j; Z_j\})$ at the point r_i, induced by the electric field due to lattice distortions, with the electric field itself, and which is therefore a function of the inverse fourth power of the interatomic distance. Because of symmetry the electric field vanishes at the ideal ionic positions in the total absence of lattice distortions; therefore the term $\mathcal{E}_{pol.}$ is zero in pure compounds. We neglect distant-neighbour interactions, three-body terms, and Van der Waals and higher-order multipole electrostatic interactions.

The infinite system is described using periodically repeated supercells. It is useful to express the ionic positions $\{\boldsymbol{r}_i\}$ in terms of the ideal undistorted positions based on the average lattice parameter a and of the displacements $\{\delta\boldsymbol{r}_i\}$ from such positions. The equilibrium configuration of the distorted alloy is obtained by minimizing the total energy $\mathcal{E}$ with respect to the parameters a and $\{\delta\boldsymbol{r}_i\}$. An efficient minimization procedure has been followed taking into account that (i) the energy is very sensitive to small changes in the average lattice parameter a, and less sensitive to the ionic displacements and, (ii) in the equilibrium configuration the sublattice containing the common ions shows larger relaxations—since the NN ions are different—than the other sublattice.

We simulate the infinite alloy using periodically repeated simple cubic, face-centred cubic, or body-centred cubic supercells (which we indicate with SC, FCC, and BCC respectively), having therefore the cubic symmetry which characterizes the Bravais lattice of the constituent pure compounds. The supercells are filled with the different anions and cations according to (i) cubic symmetry or (ii) a random distribution.

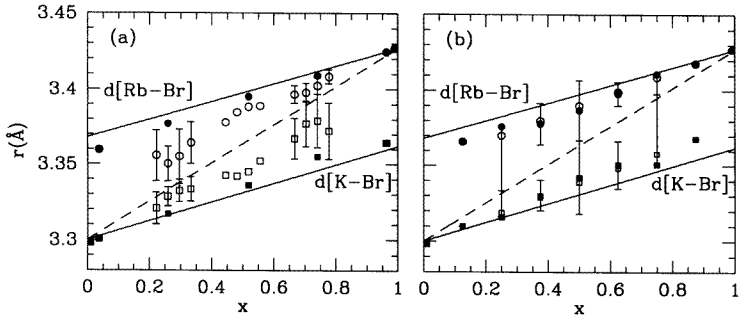

Figure 1. NN distances in $K_{1-x}Rb_xBr$ alloy, calculated using a 54-atom FCC cell with cubic symmetric filling (panel (a)) and a 16-atom FCC cell with random filling (panel (b)). Circles and squares refer to d[Rb–Br] and d[K–Br] respectively; the results averaged over all the different configurations allowed in the supercell for a given composition are shown by open symbols, their spreading (if present) is indicated by the error bars, and the results for the SQS configuration are represented by solid symbols. Solid lines indicate the experimental data [2], and the dashed line shows the NN distance obtained from the alloy average lattice parameter, which follows the Vegard law.

Following the first scheme, the ions are grouped into shells of symmetry-equivalent positions, each one filled by one kind of ion. The cubic symmetric filling prevents random lattice distortions: the allowed displacements are radial relaxations of the shells, so that the equilibrium geometry is fully described by the alloy average lattice parameter a and by few independent distortion parameters (one for each shell which can relax). In the preliminary work reported in [11], only the minimum cell of this kind allowing for internal distortions was considered. It is a FCC cell with 16 atoms describing the alloy with composition $x = 1/8$ or $7/8$: it corresponds only to one possible configuration (i.e. distribution of

ionic types) and it is characterized by one independent distortion parameter. We are going to consider here larger supercells, allowing for different compositions and, for each composition, for different configurations which can be inequivalent for the filling pattern and, consequently, total energies and structural equilibrium geometries.

In the case of random filling, for a given composition the number of different possible configurations and of independent distortion parameters is higher than in the case of symmetric filling (even the 16-atom FCC supercell allows for several compositions and inequivalent configurations), and increases tremendously with the size of the supercell. The computational cost of sampling all the different configurations can be drastically reduced by considering only some highly representative configurations, i.e. SQS configurations, proposed by Zunger *et al* [13] and successfully applied to the electronic properties of covalent alloys. We address the reader to the original papers for details, and we only summarize here the basic concepts necessary to understand our application. The SQS's configurations are those particular configurations which have the highest statistical weight and whose energy better approximates that of the completely random alloy. In general (for a given cell and composition) only one SQS configuration exists, but in some particular cases there are several inequivalent SQS configurations with the same energy.

3. Applications to $K_{1-x}Rb_xBr$

In this section we discuss in some detail the application of the model to the $K_{1-x}Rb_xBr$ alloy. We set the repulsive potential parameters B and ρ in order to reproduce the experimental NN interatomic distances in the pure compounds: 3.298 and 3.427 Å in KBr and RbBr respectively [5], corresponding to a lattice mismatch of about 4%. A significant test concerning our energy model is the study of extreme dilutions, i.e. of the limiting cases $x \to 0$ and $x \to 1$. With this aim, we have considered supercells with only one substitutional impurity, i.e. $x = 2/N$ or the complementary case $x = 1 - 2/N$, where N is the number of atoms for the supercell. These particular fillings have the same cubic symmetry of the supercell. We found that a 128-atom FCC cell is large enough to simulate the isolated impurity limit, with $x = 1/64$ (or the complementary case $x = 63/64$): among the shells of ions surrounding the substitutional impurity, in fact, the first shell shows significant distortions, whereas the second and the third ones are already only slightly distorted. The radial relaxation $|\delta \boldsymbol{r}|$ of the first shell is about 0.06 Å away from the impurity for $x \to 0$ and conversely towards the impurity for $x \to 1$; the relaxation of the second and third shells is one order of magnitude smaller, and that of the others even less. The average lattice parameter is very close to the Vegard prediction and to the experimental data. The calculated NN distances between the substitutional ion and the common one are slightly different with respect to the experimental values, and in both cases between the corresponding Vegard value and the experimental one: we obtain d[Rb–Br] = 3.362 Å for $x \to 0$, and d[K–Br] = 3.363 Å for $x \to 1$, whereas the corresponding experimental data are 3.368 and 3.362 Å respectively (figure 1(a)). The agreement between our predictions and the experimental data for the isolated impurity limit is good enough to make us confident about the validity and the applicability of the model to intermediate compositions. In what follows, we present and compare the results obtained using different supercells with the two different filling criteria illustrated above.

Among the symmetric-filled supercells, we focus mainly on a 54-atom FCC cell, allowing for several compositions and configurations (we address the reader to [11] for the 16-atom FCC supercell). In figure 1(a) we show the variation of the NN distances in the alloy, obtained using this cell. For each composition we show the results obtained

for d[K–Br] (open squares) and d[Rb–Br] (open circles), averaged over the different configurations allowed, equally weighted, and—for each configuration—over the various distances present in the supercell. The error bars indicate the spreading of the average NN distances over the different configurations eventually allowed. The alloy average lattice parameter is always close to the Vegard value and it is not reported in the figure.

We have also considered for comparison a 64-atom SC cell. The results obtained are similar to those obtained with the 54-atom FCC cell. Remarkably, the 64-atom SC cell with symmetric filling can be used to describe several configurations for the compositions $x = 1/8$ and $x = 7/8$, previously studied [11] in only one configuration with the small 16-atom FCC cell. We found that the NN distances averaged over all the configurations allowed in the 64-atom SC cell are worse than the values obtained with the single configuration of the small 16-atom FCC cell: this is because the average for the 64-atom SC cell includes also unrelaxed configurations, where the internal distortions are symmetry forbidden.

This example points out that the results obtained with the cubic-symmetric filling must be evaluated globally over the entire range of compositions studied and supercells used; in fact a given supercell can be more suitable to describe some compositions rather than others, and can give misleading results for those specific compositions that admit many configurations with symmetry-forbidden internal distortions. We can however conclude that globally the use of larger supercells better simulates the random system allowing in general for many relaxed configurations and many independent distortion parameters. In summary, comparing the results obtained with the symmetrically filled cells with the experimental data, we observe that the agreement is satisfactory for compositions x close to 0, 0.5, and 1, but at variance with other intermediate compositions.

In order to investigate whether the discrepancy with the experimental data is mainly due to the particular filling criterion, or if it is an intrinsic limit of the energy model, we consider the case of random filling. In this case even a small supercell allows for many compositions. For instance the 16-atom FCC cell can describe the alloy with $x = n/8$, where $n = 1, 2, \ldots, 7$. In figure 1(b) we show the results for the NN distances, using the same symbols as panel (a). Also in this case, for each composition the average lattice parameter is close to the Vegard value and it is not reported in the figure. In both panels (a) and (b) we also show the NN distances obtained from the SQS configurations (solid symbols; in panel (a) we do not report all those possible with the 54-atom cell, but only those for some selected compositions). One can see that in general the NN distances obtained with the SQS configuration are close to the results averaged over the different configurations with random filling, as assessed in [13].

We find it instructive at this point to discuss in some detail the results obtained for compositions $x \approx 0.5$, for which the comparison between the symmetric and random filling criteria could be quite meaningful; for the extreme concentrations, conversely, we expect that randomly and symmetrically filled cells give many identical configurations, and therefore no very different results. In figure 2 we report the results obtained from (a1) the average of the symmetric filling configurations for a 54-atom FCC cell ($x \approx 0.52$), (a2) the SQS configuration for the same cell and composition, (b1) the average of the random filling configurations for a 16-atom FCC cell ($x = 0.5$), and (b2) the SQS configuration for the same cell and composition. Whereas the average values (solid lines) of the d[Rb–Br] and d[K–Br] NN distances in the different cases are quite similar, non-negligible differences occur in their statistical distributions. The distributions of d[Rb–Br] and d[K–Br] are rather broadened (the maximum broadening occurring in the case (a1), i.e. for the cubic symmetrically filled supercell) and partially overlapping. They cover a range including both the corresponding bulk value (long-dashed line) and the unrelaxed NN distance as

deduced from the average lattice parameter of the alloy (dotted line); the average value of the distribution is intermediate between these values.

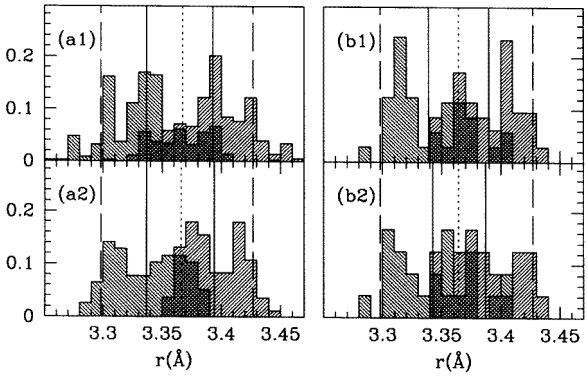

Figure 2. NN distance distribution in $K_{1-x}Rb_xBr$ alloy for $x \approx 0.5$. Panel (a1) refers to the 54-atom FCC cell with symmetric filling and $x \approx 0.52$, whereas panel (b1) refers to the 16-atom FCC cell with random filling and $x = 0.5$; panels (a2) and (b2) show the results for the SQS configurations for the same cells and compositions as the corresponding upper panels. In the upper panels the distributions are obtained by averaging over the different configurations allowed. The vertical solid lines represent the average NN distances; the long-dashed lines indicate the NN distances in the corresponding pure compound, and the dotted lines indicate the unrelaxed NN distance deduced from the alloy average lattice parameter. The distributions are normalized to one.

To briefly quantify the variation of the NN distances as a function of the alloy composition it is useful to introduce the ratio

$$\eta(x) = \frac{d[\text{Rb–Br}](x) - d[\text{K–Br}](x)}{d[\text{Rb–Br}](1) - d[\text{K–Br}](0)} \tag{2}$$

where d[Rb–Br](1) and d[K–Br](0) are the bulk values. Since d[Rb–Br](x) and d[K–Br](x) have a similar linear behaviour, η is almost constant with x and can be extracted with a fit over the entire range of composition. The value $\eta = 0$ would indicate that the lattice is undistorted and that the NN distances have the common value predicted by the Vegard law, whereas $\eta = 1$ would describe the case in which the NN distances conserve their own bulk values. We find from the experimental data $\eta^{exp.} = 0.53$, a value which is typical for the ionic compounds, whereas in the covalent alloys η is closer to 1 [15]. From the different sets of calculated NN distances, we obtain $\eta = 0.27$ when estimated from the results of the 54-atom FCC cell with symmetric filling, 0.47 from the SQS configurations of the same cell, and 0.43 from the results of the 16-atom FCC cell with random filling, as well as from the SQS configurations of the same cell. We are confident that the agreement with the experimental data could be improved with a limited computational effort using SQS configurations in larger supercells.

We conclude the analysis of our results looking at the cation–cation and anion–anion NNN distances and related distributions. We focus on the SQS configuration for $x \approx 0.52$ in the 54-atom FCC cell. The distributions of the four different kinds of NNN distance, namely K–K, Rb–Rb, K–Rb, and Br–Br, are shown in figure 3. The Br–Br NNN distances have a quite broadened distribution, although peaked around the unrelaxed distance deduced from the average alloy lattice parameter; a similar broadening is present also for the distances between higher-order neighbours. Conversely, all the cation–cation distance distributions

are rather sharp. These results are in agreement with the trends extracted from the EXAFS data, and can be easily understood considering that the common ion (i.e., Br in this case) sublattice shows the most relevant distortions.

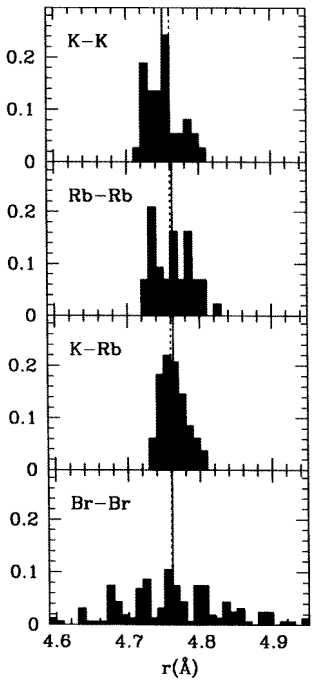

Figure 3. NNN distance distributions in the random $K_{1-x}Rb_xBr$ ($x \approx 0.52$) alloy simulated with the SQS configuration in a 54-atom FCC cell. The results are presented for all the different pairs of NNNs, i.e. for K–K, Rb–Rb, K–Rb, and Br–Br from the uppermost to the lowest panels. The solid line is the average of the distribution, and the dashed line indicates the value deduced from the alloy average lattice parameter. The distributions are normalized to one.

4. Other ionic alloys and conclusions

We apply our model also to $RbBr_{1-x}I_x$ and $KCl_{1-x}Br_x$ alloys, for which EXAFS data are reported in detail in [1] and [5]. For $K_{1-x}Na_xCl$ and $K_{1-x}Na_xBr$ not many details are given in the related reference [3]. The trends obtained from the calculated NN and NNN distances are similar to those previously discussed for $K_{1-x}Rb_xBr$, but the agreement with the experimental data is worse. In fact, we find a disagreement even for the impurity limits. For $RbBr_{1-x}I_x$ we obtain d[Rb–I] = 3.541 Å for $x \to 0$, and d[Rb–Br] = 3.532 Å for $x \to 1$, whereas the experimental data are 3.591 and 3.518 Å respectively. For the other alloy, $KCl_{1-x}Br_x$, we obtain d[K–Br] = 3.177 Å when $x \to 0$ (3.195 Å experimentally) and d[K–Cl] = 3.172 Å when $x \to 1$ (no experimental data are available). For this alloy discrepancies between our predictions and the experimental data also exist for intermediate compositions.

In order to understand whether those discrepancies are due to the simplicity of the energy model used, we performed *ab initio* pseudopotential [16] calculations for the $RbBr_{1-x}I_x$ alloy at some selected compositions in small supercells. At variance with our simple

model, such calculations take properly into account the electronic charge distribution, and therefore include corrections both to the Madelung electrostatic energy (which accounts for pointlike charge–charge interactions only) and to the short-range repulsive energy; also NNN interactions are included, whereas Van der Waals interactions are not. For a given supercell, composition, and configuration, the results obtained from the model and from the *ab initio* calculations are not significantly different, supporting therefore the validity of the energy model used, despite its simplicity.

However, we have also considered the possibility of refining the model including NNN repulsion [17] and Van der Waals [18] and three-body [19] interactions. We studied the effect of each term separately, considering the SQS configuration in the 16-atom FCC cell. We found that the addition of these terms as well as small changes in the parameters involved in the model (i.e. ionic polarizability [20] and repulsive parameters) do not affect significantly the final results, and in particular do not improve the agreement with the experimental data. We point out that not only is the polarization term very important, as already observed in [11], but it is really the only term relevant to our purposes. We think that a possible source of discrepancy between our results and the experimental data in some systems can be the temperature at which the data are detected. In [21] a large variation of η is reported for the $AgBr_xCl_{1-x}$ ionic alloys: η changes from ≈ 0.55 to ≈ 0.87 when the temperature increases from 77 to 295 K, thus indicating that low-temperature conditions, as in the case of our model, are characterized by small values of η. Unfortunately, no experimental data on the temperature dependence of η for the systems that we have investigated here are available to support this idea.

References

[1] Boyce J B and Mikkelsen J C 1984 *EXAFS and Near Edge Structure III* ed K O Hodgson, B Hedman and J E Penner-Han (Berlin: Springer) p 426
Boyce J B and Mikkelsen J C 1985 *Phys. Rev.* B **31** 6903

[2] Frenkel A, Stern E A, Voronel A, Quian M and Newville M 1993 *Phys. Rev. Lett.* **71** 3485
Frenkel A, Stern E A, Voronel A, Quian M and Newville M 1994 *Phys. Rev.* B **49** 11 662

[3] Murata T, Matsukawa T and Naoe S 1988 *Solid State Commun.* **66** 787
Murata T, Matsukawa T and Naoe S 1989 *Physica* B **158** 610

[4] Sato H, Yokoyama, Ono I, Kaneyuki K and Ohta T 1992 *Japan. J. Appl. Phys.* **31** 1118

[5] Murata T 1984 *EXAFS and Near Edge Structure III* ed K O Hodgson, B Hedman and J E Penner-Han (Berlin: Springer) p 432

[6] Vegard L 1921 *Z. Phys.* **5** 17

[7] Königsberg E and Schrunner H 1989 *Phys. Status Solidi* b **151** 101
Maity S N, Roy D and Sengupta S 1980 *Phys. Status Solidi* b **99** 327
Cox A and Sangster M J L 1985 *J. Phys. C: Solid State Phys.* **18** L1123
Maity S N and Roy D 1984 *Phys. Status Solidi* b **122** 449
Krishnamurthy C V and Murti Y V G S 1986 *Phys. Rev.* B **34** 8922

[8] Maity S N, Sengupta S and Roy D 1989 *Phys. Status Solidi* b **156** 83

[9] Fujikawa T, Okazawa T, Yamasaki K, Tang J C and Murata T 1989 *Physica* B **158** 365

[10] Fukay T 1985 *Japan. J. Appl. Phys.* **23** L208
Fukay T 1985 *J. Appl. Phys.* **57** 5188
Shih C K, Spicer W E, Harrison W A and Sher A 1985 *Phys. Rev.* B **31** 1139
Hardy J R and Karo A M 1979 *The Lattice Dynamics and Statics of Alkali-Halide Crystal* (New York: Plenum)
Tan Y T and Lushington K J 1993 *J. Phys. Chem. Solids* **54** 309

[11] Peressi M and Baldereschi A 1987 *Solid State Commun.* **63** 91
Baldereschi A and Peressi M 1993 *J. Phys.: Condens. Matter* **5** B 37

[12] Tosi M P 1964 *Solid State Physics* vol 16, ed F Seitz and D Turnbull (New York: Academic) p 1 and references therein

[13] Zunger A, Wei S-H, Ferreira L G and Bernard J E 1990 *Phys. Rev. Lett.* **65** 353
Wei S-H, Ferreira L G, Bernard J E and Zunger A 1990 *Phys. Rev.* B **42** 9622
[14] Tessman J R, Khan A K and Shockley W 1953 *Phys. Rev.* **92** 890
[15] As pointed out in the experimental literature, the difference has to be ascribed to the different type of bonding and the corresponding strength of the interaction parameters.
[16] Buongiorno Nardelli M, Baroni S and Giannozzi P 1995 *Phys. Rev.* B **51** 8060
[17] Cubicciotti D 1961 *J. Chem. Phys.* **31** 1646
Cubicciotti D 1960 *J. Chem. Phys.* **33** 1579
Cubicciotti D 1961 *J. Chem. Phys.* **34** 189
Shanker J and Agrawal D P *Phys. Status Solidi* b **98** 535
[18] Shanker J, Agrawal G G and Singh R P 1978 *J. Chem. Phys.* **69** 670
[19] Löwdin P O 1947 *Ark. Mat. Astr. Fys.* **35A** 30
Lündqvist S O 1955 *Ark. Fys.* **9** 435
Garg V K, Puri D S and Verma M P 1977 *Phys. Status Solidi* b **80** 63
Cochran W 1971 *CRC Crit. Rev. Solid State Sci.* **2** 1
Singh R P and Shanker J 1979 *Phys. Status Solidi* b **93** 373
[20] Dutt N, Agrawal G G and Shanker J 1985 *Solid State Commun.* **55** 993
Mahan G D 1986 *Phys. Rev.* B **34** 4235
[21] Yokoyama T, Takamatsu F, Seki K, Miyake K, Tani T and Ohta T 1990 *Japan. J. Appl. Phys.* **29** L1486